24th COBEM - 2017

24th ABCM International Congress of Mechanical Engineering
December 3-8, 2017, Curitiba, PR, Brazil

COBEM-2017-0568
VISCOUS EFFECTS ASSESSMENT THROUGH NONLINEAR LIFTING-LINE THEORY

Jose Rodolfo Chreim
Universidade de Sao Paulo, 380 Professor Luciano Gualberto Ave. - Butanta, Sao Paulo/SP
jrchreim@usp.br
Joao Lucas Dozzi Dantas
Instituto de Pesquisas Tecnologicas do Estado de Sao Paulo, 532 Professor Almeida Prado, Ave. - Butanta - Sao Paulo/SP
jdantas@ipt.br
Karl Peter Burr
Fundacao Universidade Federal do ABC - 5001 dos Estados Ave. - Santa Terezinha - Santo Andre/SP
karl.burr@ufabc.edu.br
Marcos de Mattos Pimenta
Universidade de Sao Paulo, 380 Professor Luciano Gualberto Ave. - Butanta, Sao Paulo/SP
mmpimenta@uol.com.br

Abstract. *An existing extension to the classic Prandtl's Lifting-Line theory is assessed for viscous effects. The method incorporates two preeminent differences from the original formulation: (i) a nonlinearization of the constitutive equations and (ii) the incorporation of viscosity through the use of bi-dimensional aerodynamic data from XFOIL. Three cases were tested to verify and validate the tool; both convergence study and comparison with another numerical method and experimental data are presented. In general, the lift coefficient is in good agreement for small angles of attack and, as it increases, this quantity deviates from one method to the other. Moreover, for the straight wing, the stall occurs at different angles of attack. In terms of drag, the coefficient agrees well for the straight wing, while it doesn't for the elliptical one. Nevertheless, the agreement is worst at small angles for both cases. A 45-degree sweptback wing is also evaluated, and the convergence analysis indicates that the proposed formulation is not suitable. Finally, the formulation seems to be powerful as a preliminary wing design tool, given the necessary improvement suggestions made.*

Keywords: *Aerodynamics, Wing design, Lifting-line, Viscous effects.*

1. INTRODUCTION

The first model to predict the aerodynamic behavior of wings was developed by the scientist Ludwig Prandtl and his colleagues from 1911 to 1918 (Anderson Jr, 2010). Prandtl's Lifting-Line Theory (LLT) is a potential flow based theory that consists of representing a real wing by a superposition of spanwise 'horseshoe vortices', elements of constant circulation Γ formed by four segments: a 'bound vortex' or 'lifting-line', generally lying on the wing planform at its quarter-chord line, two 'trailing vortices' starting from the bound vortex and extending far downstream and a 'starting vortex' located at infinity. A horseshoe vortex is depicted on Fig. 1: the bound vortex is the segment BC, the two trailing vortices are the segments AB and CD and the starting vortex is represented by the segment DA. Q_∞ is the free stream velocity. The representation of the wing by the LLT is presented in Fig. 2, in which an infinite number of infinitesimal-strength horseshoe vortices is used.

With this formulation, it is possible to calculate the induced velocity anywhere in the flow-field using Biot-Savart's law for aerodynamics. Considering a flat plate section and a zero local normal velocity component boundary condition at the three-quarter chord location (more commonly known as 'Pistolesi Boundary Condition' - PBC), an expression known as *Prandtl's Fundamental Equation* is obtained in terms of the various angles of attack. After making the adequate assumptions, the final expression is an integro-differential equation which must be satisfied throughout the wing and whose solution provides its circulation distribution (Katz and Plotkin, 2001) (Note that this is one of the possible ways of obtaining *Prandtl's Fundamental Equation*). Prandtl's LLT is surprisingly simple and elegant, bringing insightful results; its development was a keystone for further advances in modern aerodynamics. However, as the use of LLT is limited, several adaptations have been developed, broaden its application to more complex wing geometries and to incorporating effects of non-linear aerodynamics.

In 1947, Weissinger (1947) proposed one of the most important adaptations of Prandtl's LLT. Called 'vortex-step method' or 'Weissinger's method', the wing is discretized by means of several horseshoe vortices placed side by side as

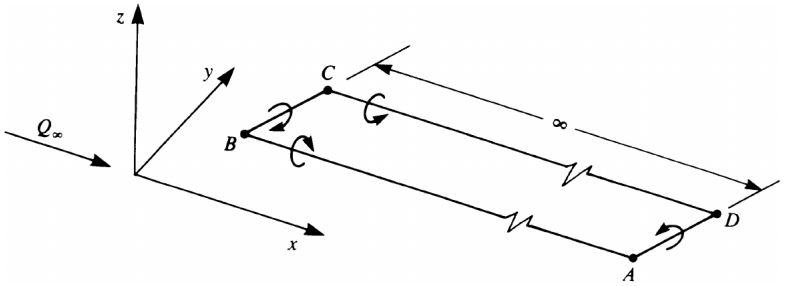

Figure 1. A typical horseshoe element, consisting of a bound vortex (segment BC), two trailing vortices (segments AB and CD) and a starting vortex (segment DA). Q_∞ is the free stream velocity. From Katz and Plotkin (2001)

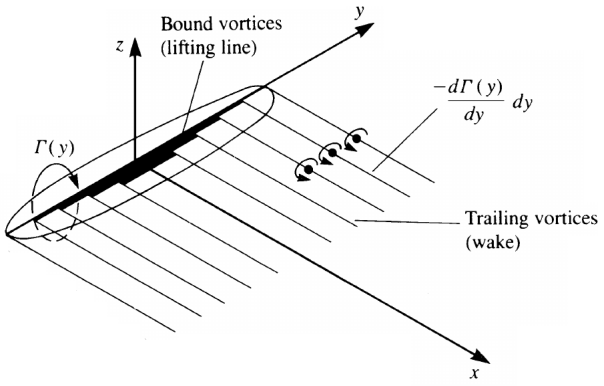

Figure 2. Wing discretization by a superposition of various constant strength horseshoe vortices in Prandtl's LLT. $\Gamma\,(y)$ is the value of the circulation as function of the span. From Katz and Plotkin (2001)

opposed to superposing one horseshoe vortex over another (Fig. 3). Still imposing the PBC, this formulation is capable of solving for flows over non-symmetrical wings or with unconventional planform.

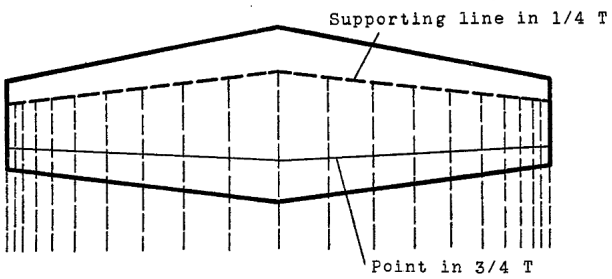

Figure 3. Wing discretization by placing several constant strength horseshoe vortices side by side for Weissinger's method. FRom Weissinger (1947)

Anderson and Corda (1980) adapted the classic formulation into a numerical iterative scheme so that nonlinear airfoil lift coefficient data could be used. In their formulation, a new circulation distribution is calculated from Kutta-Joukowski theorem and the mathematical definition of lift coefficient. Even though the numerical method still considers the location of the control points at the three-quarter chord line, the PBC is not applied anymore. Instead, it is proposed a force equivalence between that obtained by the vortex lifting law and from the definition of lift coefficient.

Owens (1998) combined the Weissinger's method along with Anderson's nonlinear formulation in order to develop what later became known as 'Weissinger's non-linear lifting line method'. Using experimental C_n and C_c data, the author claims to obtain accurate results in comparison to experimental data. Furthermore, the method seems to work for swept and tapered wings. As a drawback, non-unique numerical solutions were found in post-stall regions.

Having interest in modelling more complex geometries, Prössdorf and Tordella (1991) suggested a bound vortex distribution that allowed for curved geometries. Their formulation served as basis for Wickenheiser and Garcia (2007) to extend the LLT to analize blended-wing bodies. In a different manner than Owens (1998), the authors used the ideas of DeYoung (apud Wickenheiser and Garcia, 2007) to consider real data from airfoils. In a later work, however, Wickenheiser

and Garcia (2011) incorporated Owens' methodology to show that the numerical results corroborate experimental data for small incidence angles of attack. Moreover, they were able to correctly predict the angles at which stall ocurred.

Meanwhile, a novel lifting-line method was presented by Phillips and Snyder (2000). The method was based on a three-dimensional vortex lifting law and, according to the authors, could be used for systems of lifting surfaces with arbitrary geometry. The authors have used a discretization similar to that of Weissinger's; the control points, however, were placed at the bound vortices (quarter-chord line) and the free-wake vortices are shed in the direction of the free-stream. The formulation also imposes a force equivalence at the control points, with the difference that the obtained nonlinear system is solved by Newton's method. Finally, instead of representing the circulation distribution by a Fourier Series, Γ is represented by constant discrete values at each station, as in Fig. 4. This representation is somewhat beneficial in the sense that a system of algebraic equations with the dimension of the number of control points used for the discretization is obtained straightforwardly, without any further assumption. The viscous effects are incorporated through the sectional lift coefficient C_n, priorly obtained either experimentally or numerically.

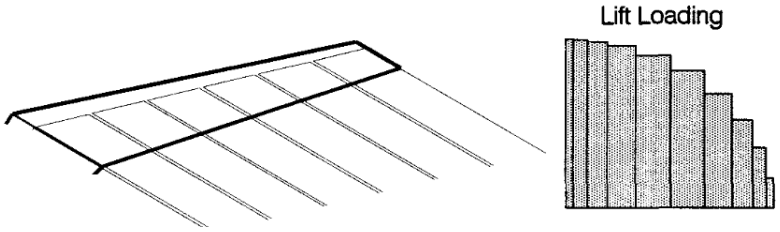

Figure 4. Representation of circulation Γ in the method proposed by Philips. Adapted from Barnes (1997) and Phillips and Snyder (2000)

In this work, an evaluation of the viscous effects on flow past wings is presented using the lifting-line methodology proposed by Philips. The numerical tool was developed in MATLAB environment with XFOIL panel code used to generate the C_n and C_c database as function of the angle of attack, Mach number, Reynolds number and airfoil geometry. The next sections concern to the developed methodology, numerical results containing a convergence study and subsequent comparison with experimental data and other numerical methods, and a conclusion of the work along with future work.

2. METHOD

For the geometry of the wing, chord, geometric twist, span, and sweep distributions are inputs, as well as the number of control points N for the discretization along with the respective airfoil section. For the flow condition, inputs are free stream Reynolds number Re_∞ (although not used for inviscid flows, the free stream velocity V_∞ is calculated based on Re_∞), geometric angle of attack α, and type of flow (potential, compressible, viscous, or full regime). Air properties such as dynamic viscosity, density rho, static temperature, gas constant and pressure to volume specific heat ratio are pre-defined. Along with V_∞, the speed of sound and free stream Mach number, when applicable, are calculated.

The coefficient $\frac{\partial C_n}{\partial \alpha}(y)$ is initially assumed to be of a flat plate, i.e., 2π. From this assumption, and neglecting the nonlinear terms of the governing equations, an initial estimate for the circulation distribution $\Gamma(y)$ is obtained.

Data for the lift and drag coefficients, C_n and C_c respectively, are loaded based on the chosen airfoil sections, Mach M and Reynolds Re range of values. XFOIL is used to calculate virtually every sectional information needed, besides the geometry itself. Additionally, within MATLAB environment, interpolating functions are generated from the data to interpolate any arbitrary combination of α, M, and Re for a given airfoil.

For each wing station, a force equivalence condition is applied: the aerodynamic force calculated by the Kutta-Joukowski theorem is compared to the aerodynamic force calculated using the C_n definition, according to the following equation:

$$\rho\Gamma|\vec{V}\times\delta\vec{l}| = \frac{1}{2}\rho V_\infty^2 C_n \bar{c}\delta l \tag{1}$$

In which $\vec{V}$ is the total velocity at a control point (in vector form), $\bar{c}$ the aerodynamic mean chord length for the wing section, and $\delta\vec{l}$ the spatial vector along the bound segment (δl is its norm). It is verified whether equation (1) is satisfied to within some tolerance. If tolerance is not satisfied, an iterative process starts. A corrector vector $\Delta\Gamma$ is calculated using multi-dimensional Newton-Raphson method and the value of Γ is updated. Then, all necessary variables are recalculated. When convergence is reached, Γ, C_n, and C_c distributions are stored. The wing aerodynamic coefficients C_L and C_D are calculated and the script exits. Note that C_L and C_D are formed by contributions of both C_n and C_c, meaning that the method takes into account the lift and viscous drag effects from 2-D data to calculate the overall wing coefficients. The methodology is carefully explained on Phillips and Snyder (2000) and is illustrated in the following flowchart:

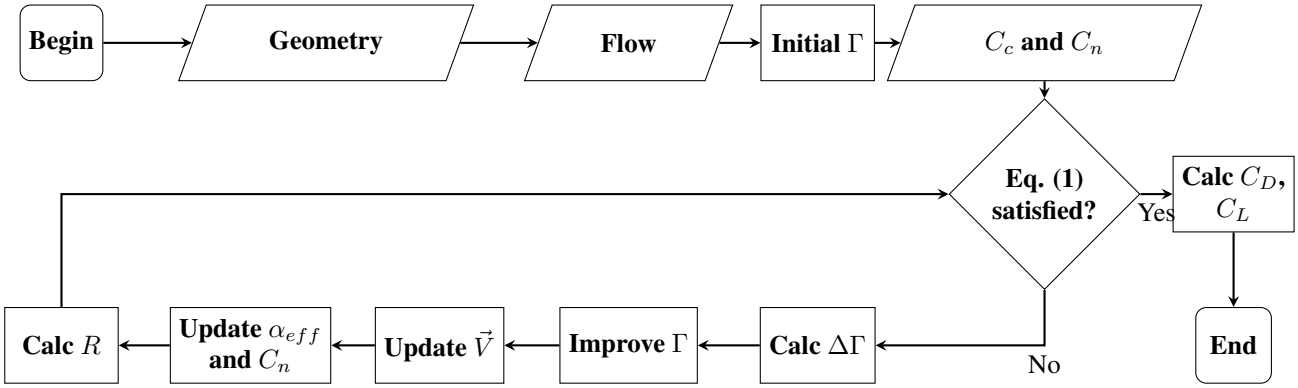

3. RESULTS

This section is divided into two subsections: the former is a convergence study for three wings in order to assess the effects of mesh refinement on the numerical solution. The latter is a comparison of the nonlinear lifting-line with experimental and numerical data, obtained from the literature and the Star-CCM+ Computational Fluid Dynamics (*CFD*) software, respectively.

3.1 Mesh convergence study

Prior to the comparison with the experimental and numerical data, a convergence study was conducted to verify the tool and also to check its accuracy. Three wings were evaluated: (i) a flat-plate elliptical planform wing under potential flow, (ii) a NACA 0012 straight planform wing under viscous flow and (iii) a flat-plate $45°$ sweptback wing under potential flow. They are summarized on the following table and their planforms are presented on Fig. 5.

Table 1. Geometric and flow properties for the first convergence study case

Flow properties	Case I	Case II	Case III
Planform	Elliptical	Straight	Straight
Wing Section	Flat plate	NACA 0012	Flat plate
span 'b' (m)	2.0544	5.900	2.4892
chord root 'c_0'(m)	0.3566	1.00	0.5080
Sweep angle 'Λ' (deg)	0	0	45
Free stream velocity 'V_∞' $\left(\frac{m}{s}\right)$	74.68	49.67	51.81
Geometric angle of attack 'α' (deg)	8	8	8

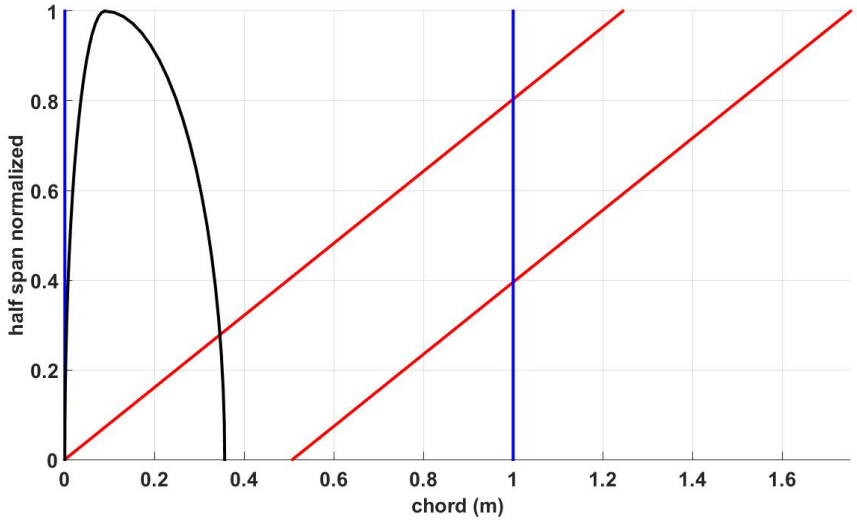

Figure 5. Wing planforms used in the study: Case I: Black lines. Case II: Blue lines. Case III: Red lines. The free stream velocity comes from west to east.

This study was conducted increasing the number of horseshoe vortices and checking the convergence of C_L. The number N of horseshoe vortices per semi-span varied from 28 to 904, increasing consecutively by a value of approximately $\sqrt{2}$, value based on experience rather than on mathematical derivation (Committee *et al.*, 2009). The variation in N is represented by a change in the refinement ratio r, defined according to eq. (2): for $r = 1$, $N = 904$ (i.e., the most refined grid) and as $r \to 0$, $N \to \infty$ (i.e., an infinite number of horseshoes).

$$r = \frac{h_N}{h_{N_{Max}}} \tag{2}$$

h_N is a representative mesh size for N horseshoe vortices. For the case of non-structured grids, such as the case of the present formulation, h_N is defined as:

$$h_N = \frac{\sum_{i=1}^{N} \delta_{l_i}}{N} \tag{3}$$

When the finest grids were in the convergence region, the value of the extrapolated C_L, $C_{L_{ext}}$, for $r = 0$ and the discretization uncertainties were obtained through a five-step procedure for uncertainty estimation (Committee *et al.*, 2009). Also, the order of convergence p for the grids is obtained. The discretization uncertainties were calculated even for grids outside the convergence region. The fitting curves plotted along with the numerical data were obtained either using Richardson Extrapolation (elliptical and straight wings) or nonlinear least-squares (sweptback wing); thus, for the cases in which convergence occurs, numerical data being offset from the curves indicates that they are outside the convergence region. Conventional cosine clustering is generally used for its efficiency (Phillips and Snyder, 2000). For straight quarter-chord lifting lines, a denser clustering is only needed near the wing tips. According to Phillips and Snyder (2000), for wings having sweep or dihedral, however, a more refined clustering is also needed near the root due to the rapid changes in Γ arising from the discontinuity at the quarter-chord line. Figure 6 illustrates the discretization schemes.

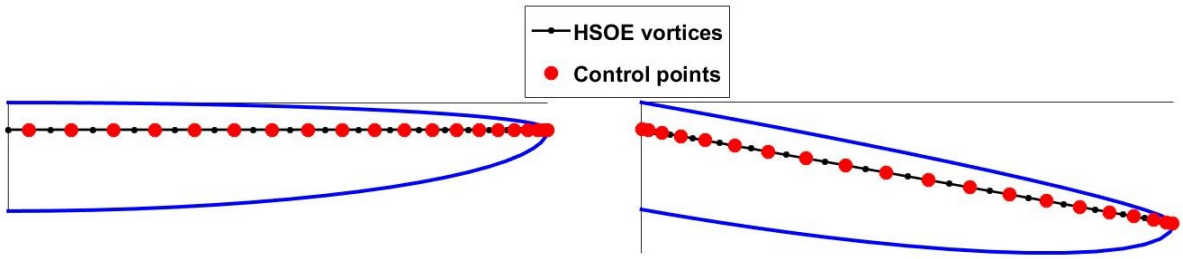

Figure 6. Clustering for a straight quarter-chord (left) and a segmented quarter-chord with $\Lambda = 10^\circ$ (right).

3.1.1 ELLIPTICAL WING UNDER POTENTIAL FLOW

The first convergence study was for a flat-plate elliptical planform wing under potential flow (Tab. 1, case I). This case was chosen due to the existence of theoretical solution (Anderson and Corda, 1980) and also to evaluate the performance of the linear solver to initialize the method.

Figure 7 shows the values for the theoretical and numerical lift coefficients C_L as the grid is refined. The graph on the right is a zoom of the graph presented on the left, evidencing the uncertainty due to discretization for the finest grid. It can be seen that C_L from the numerical method approximately converges to the theoretical value, having a 0.04 % difference from each other. Although not investigated, it is believed that the uncertainty from other numerical sources are higher than this offset. Furthermore, the rate of convergence p for this case is found to be approximately 2, the theoretical value, indicating that the numerical convergence is second order and that the C_L obtained for the finest grids are assured to be in the asymptotic region.

3.1.2 STRAIGHT WING UNDER VISCOUS FLOW

The second case was for a NACA 0012 straight planform wing under viscous flow (Tab. 1, case II). This case is interesting in order to evaluate the numerical data when effects of compressibility and viscosity are incorporated in the $C_n \times \alpha$ curve. The reason for choosing a straight planform is not to have significant variations in Re throughout the wing; a possible source of error from the solver or from the interpolating functions used to obtain an combination of (α, M, Re).

Figure 8 shows the convergence of C_L as the grid is refined. The graph on the right is a zoom of the graph presented on the left, evidencing the uncertainty due to discretization for the finest grid. The extrapolated value of C_L is approximately 0.6350 and the rate of convergence p is also found to be approximately 2; this value indicates that, for the finest grids, the method converges asymptotically even when viscous effects are incorporated through 2-D aerodynamic data.

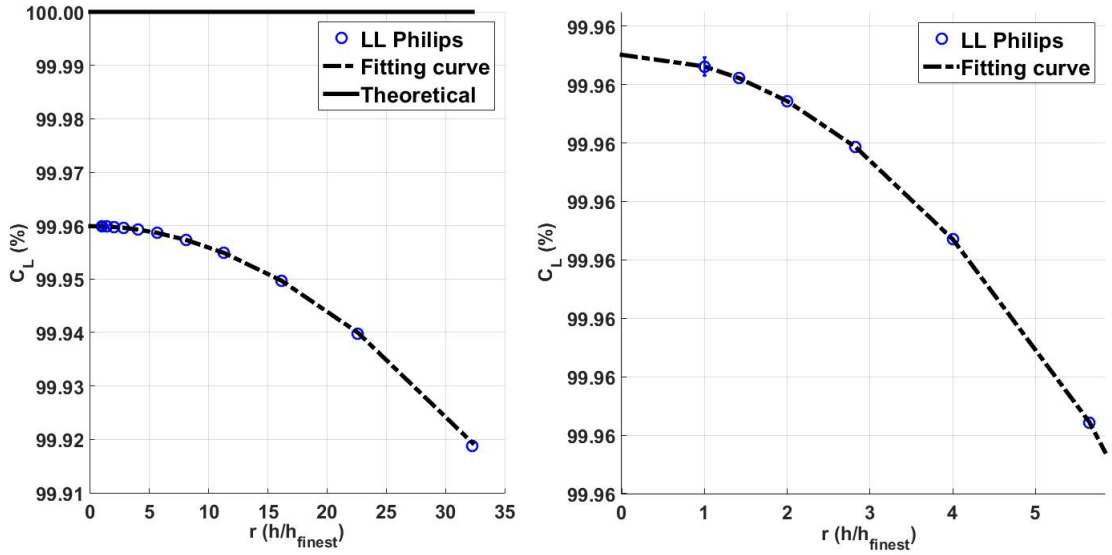

Figure 7. C_L versus r for mesh refinement study. Elliptical wing, potential flow. The blue circles represent the numerical C_L, the dash-dot line the represents the fitting curve assuming $p = 2$, and the horizontal bold line the theoretical value.

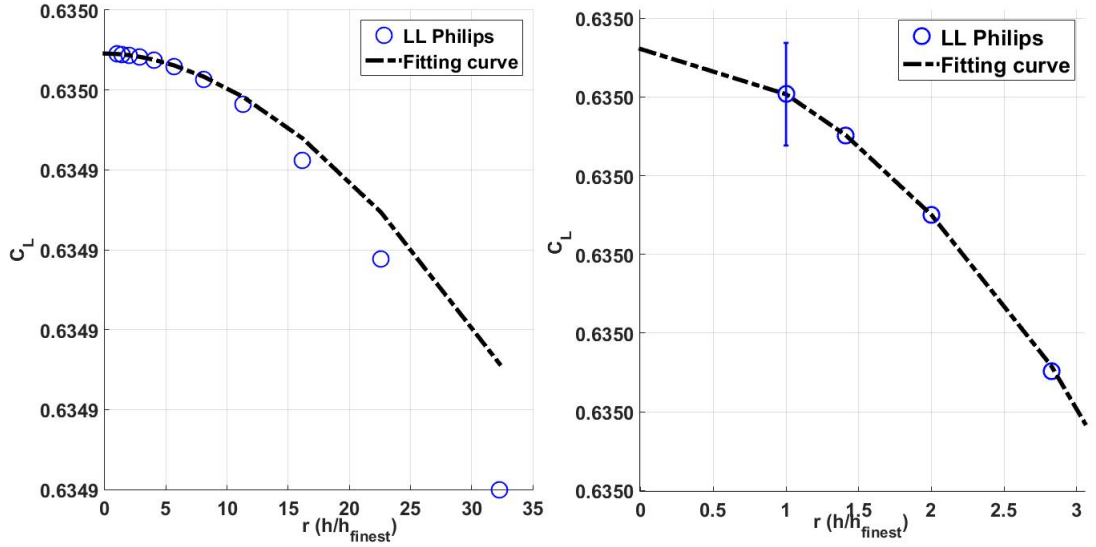

Figure 8. C_L versus r for mesh refinement study. Straight wing, viscous flow. The blue circles represent the numerical C_L, the dash-dot line the represents the fitting curve assuming $p = 2$.

3.1.3 45° SWEPTBACK WING UNDER POTENTIAL FLOW

The last case was performed for a flat-plate $45°$ sweptback wing under potential flow (Tab. 1, case III). This case is of interest in order to assess the method when three dimensional effects are more intense.

Figure 9 shows the behavior of C_L as function of r. For this case, however, a diverging trend is observed: C_L becomes higher as the grid is refined. Since the main difference among this wing and the previous ones is the quarter-chord line, the trend indicates that the present formulation might not be adequate for the case of geometries not having straight quarter-chord lines. Hunsaker and Phillips (2011) already observed this limitation for the method, proposing a reasonable explanation: by its representation, for any wing having a quarter-chord line which is not straight, such as those with sweep or dihedral, the bound vortices do not induce velocities on the control points lying on the same side of the wing. Nonetheless, they induce velocities on control points that lie on the other side. The magnitudes of these velocities become more intense as the control points become closer to the bound vortices. Hence, increasing the number of control points has the same practical effect of approximating the control points to the bound vortices on the opposite side of the wing. The effect is more prominent at the wing root due to both the cosine clustering and the proximity of the two halves of the

wing. Although the fitting curve has an order of convergence $1 > p > 0$ indicating that the solution converged (Eça and Hoekstra, 2006), the method did not work for $N = 904$ and $N = 652$. Therefore, the proposed method is not suitable for wings having discontinuities in the quarter-chord line. Note that h_{finest} was defined the same way as in the previous cases, even though the method did not converge for $N = 904$.

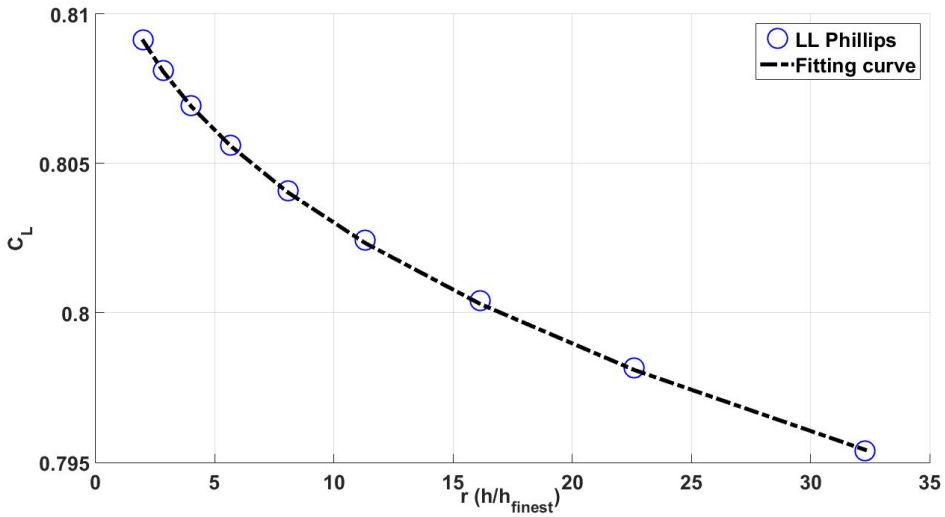

Figure 9. C_L versus refinement ratio for convergence study of a $45°$ sweptback wing under potential flow. The blue circles represent the numerical values of C_L. No convergence was attained.

As a means of ensuring convergence for the case of sweptback wings, a possible workaround is to move the control points far from the bound vortices so that the effect described is not significant. However, simply changing the control points locations does not guarantee convergence to correct values. In fact, by doing so, the boundary condition must be changed accordingly. A possible solution is to place the control points over the three-quarter chord line and to imposed a PCB, as suggested by some of the authors presented in section 1.

3.2 Comparison with experimental and numerical data

After the convergence study, it is presented a comparison of the nonlinear lifting-line method with experimental data and numerical results from Star-CCM+.

For the nonlinear lifting line method, N was set to be 904 for all the cases and discretization uncertainty estimations were performed by the same fashion as on the previous subsection. Note that the uncertainties calculated cannot be seen without zooming in the plots.

For Star-CCM+, a 2 million elements mesh half bullet-like domain was created (Fig. 10). The NACA 0012 airfoil was extruded until half span. The smallest mesh element has a characteristic length of 5.0×10^{-5} m, approximately. A symmetry condition was imposed on the lateral boundaries while inlet velocity and pressure outlet conditions were set to the front and to the back boundaries, respectively. $K - \omega$ SST turbulence model was used and the fluid was assumed to be incompressible. Although no mesh refinement study was performed to validate the results from *CFD*, wall $Y+$ was kept as close to 1 as possible and residual were within acceptable values for a 3-D simulation. For more details on the simulations for Star-CCM+, refer to Chreim (2016).

3.2.1 ELLIPTICAL WING

The elliptical wing for case I was evaluated in a viscous flow condition. The results obtained are compared to experimental data from Van Dam *et al.* (1991). NACA0012 is used throughout and the flow properties are $M_\infty = 0.2675$ and $Re_\infty = 1.70 \times 10^6$. For the experiment, boundary-layer transition was fixed on the model at 5 % of the chord over the upper and lower surfaces along the entire span, thus ensuring a virtually fully-turbulent flow. It is interesting to note that no uncertainty for experimental data were provided. Figure 11 shows the trends for both C_L and C_D as functions of the wing angle of attack.

As α increases, the simulated C_L starts gradually diverging from the experimental values. For total drag, however, the trend is the opposite: differences are more significant at lower α. The possible explanations for the differences observed are as follows: for higher angles of attack, three-dimensional effects become more prominent, trend that is not well captured by the numerical model. It is therefore expected that the C_L curve have a higher slope than the experimental counterpart. Nevertheless, even with the pointed out discrepancies, the numerical method agrees reasonably well with the

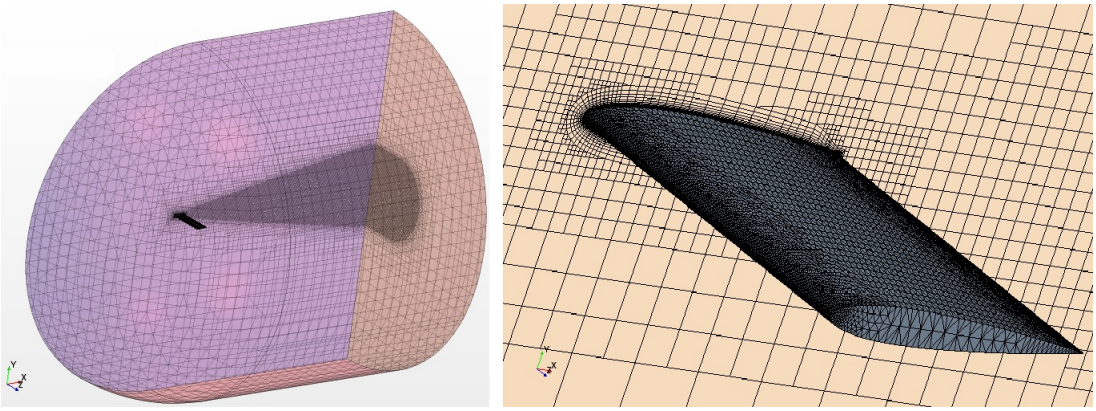

Figure 10. Left: A half bullet-like fluid domain containing approximately $3Mi$ elements under. Right: Zoomed in region showing a superficial mesh over the wing and prism layer mesh used to capture the boundary layer.

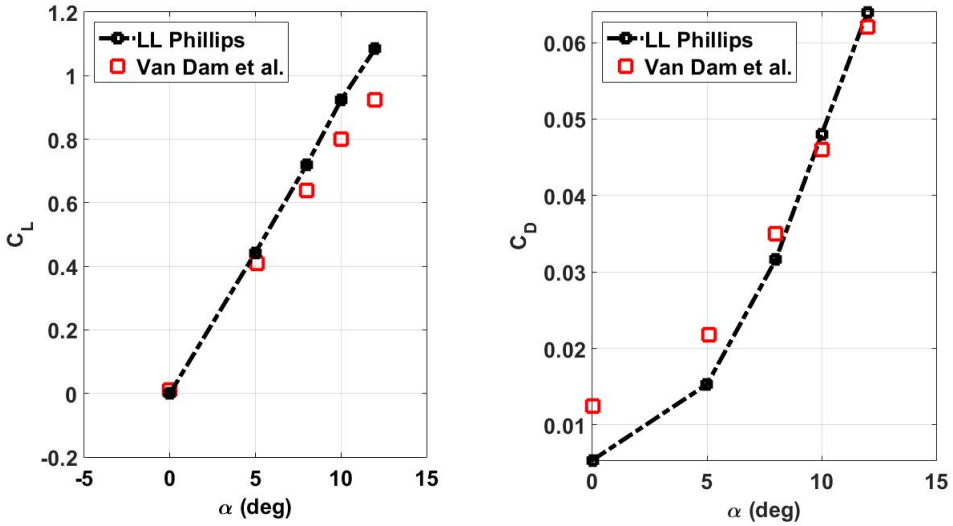

Figure 11. C_L (left) and C_D (right) versus α between experimental data (red) and nonlinear LL (black) - Elliptical wing

experimental data.

In addition to the limitations of the method to accurately capture three dimensional effects, the data for C_n and C_c obtained from XFOIL may be a source of discrepancies due to the turbulent transition model used in XFOIL; anticipating the discussion in order to corroborate the above statement, Fig. 12 shows C_n and C_c versus α for several numerical and experimental data for NACA 0012 with $Re = 6 \times 10^6$. The experimental data are from the work of Abbott and Von Doenhoff (1959) (red) and Rumsey *et al.* (2012) (blue), while the same model as on the 3-D case was kept for Star-CCM+.

XFOIL overestimates the value for C_n in comparison to almost all other data and, particularly at high angles of attack before stall, it fairly agrees with data from Abbott and Von Doenhoff (1959). C_n from Star-CCM+ are in better agreement with the tripped data due to the $k - \omega$ turbulence model. In the case of C_c, none of the data from different sources agree quite well with one another for the entire range of angles of attack; Nonetheless, for high angles of attack results from XFOIL are in good agreement with Landson (Rumsey *et al.*, 2012). This trend is essentially what is observed in Fig. 11. Therefore, the 2-D data used in the lifting-line must take into account effects of turbulence for the model to better predict turbulent flows over wings.

3.2.2 STRAIGHT WING

The straight wing for case II is used as comparison of the present lifting-line method with experiment and with Star-CCM+. The free stream Reynolds is $Re_\infty = 3.17, \times 10^6$ and the free stream Mach number $M_\infty \approx 0.15$. The experimental data are from Applin (1995): turbulence was enforced at about $5cm$ downstream the leading edge, so the flow is essentially turbulent. Figure 13 shows the trends for C_L and C_D as function of α.

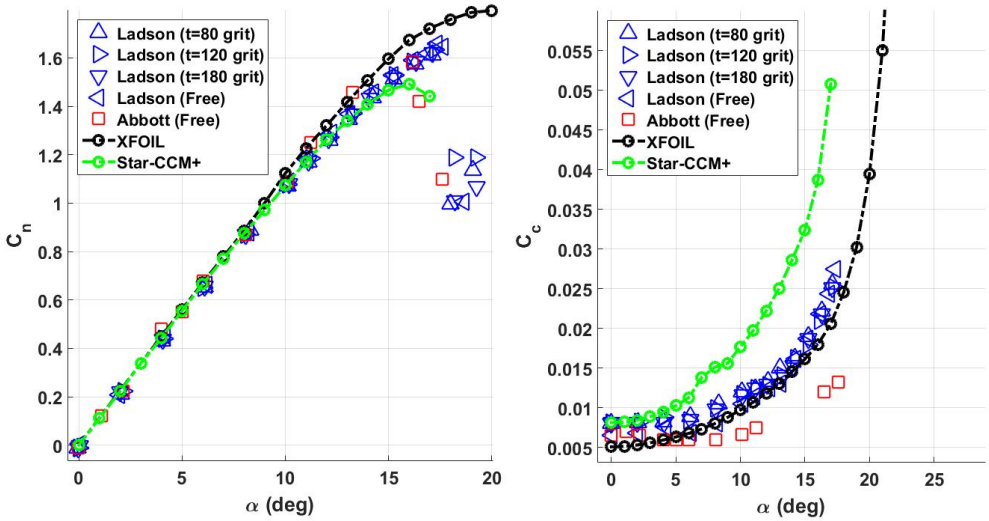

Figure 12. C_n (left) and C_c (right) versus α for experimental and numerical data. 'Free' refers to free turbulence transition, while 'grit' to enforced turbulence transition.

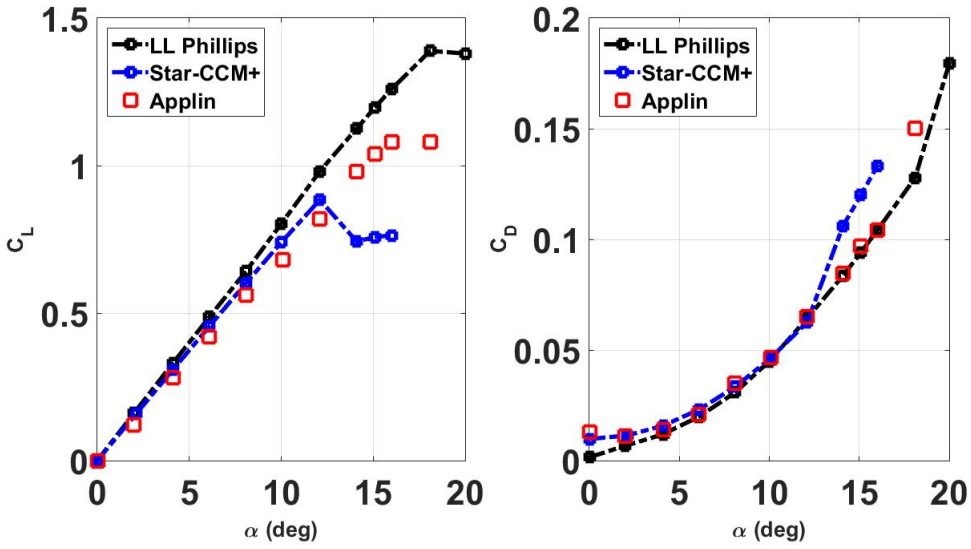

Figure 13. Comparison of C_L (left) and C_D (right) versus α among experimental data (red squares), Star-CCM+ (blue) and nonlinear LL (black) - Straight wing

Comparing C_L, satisfactory agreement happens among the three methods for small angles of attack, whereas for higher α the proposed lifting-line overestimates C_L and Star-CCM+ agrees better. However, stall occurs prematurely for Star-CCM+ and, in terms of the angle at which stall occurs, agreement seems more appropriate for the lifting-line. In light of Fig. 12 and how the numerical simulations and experiment were conducted, the results from Star-CCM+ before stall are expected to be in closer accordance with experimental data than the results from the lifting-line, as turbulence was not enforced for the 2-D data simulated on XFOIL. For C_D, Star-CCM+ has better agreement with experiment at small α, while better agreement for the lifting line starts at higher angles, even in the stalled region. This trend is once more also related to how transition to turbulence is triggered.

4. CONCLUSION AND FUTURE WORK

This work introduces a literature review of the progress of the *Lifting-Line Theory* since its early development, paying special attention to the different discretizations and imposed boundary conditions. The nonlinear methodology suggested by Phillips and Snyder (2000) is implemented along with numerical C_n and C_c airfoil data from XFOIL in order to assess the effects of viscosity on the wing aerodynamic coefficients C_L and C_D. A convergence study was performed for three wings having distinct characteristics; satisfactory convergence was observed for both the elliptical and straight planform

wings while no convergence was found for the sweptback wing. For this reason, only wings represented by straight bound-vortex distributions were suitable for comparison with experimental and numerical data. Reasonable agreement was observed for C_L, specially for small angles of incidence, while for C_D agreement is better at higher angles. These trends for C_L and C_D happened for both wings and can be partially explained by the source of C_n and C_c, whose behavior is presented on figure12, and partially by the fact that the lifting-line methodology does not take into consideration the full aspects of three-dimensional flows, which are emphasized at α.

As future work, the authors expect to obtain more reliable 2-D aerodynamic data as well as to develop a more suitable formulation which allows for the analysis of more complex geometries, such as those having sweep and dihedral angles. To do so, the transition model used in XFOIL will be carefully understood and the proposed formulation will be reconsidered; as the literature indicates, the most suitable approach for complex geometries is to have the control points placed at the three quarter chord line and to enforce the Pistolesi Boundary Condition along that location.

5. ACKNOWLEDGEMENTS

The authors would like to acknowledge the financial support and scholarship granted by the Coordenação de Aperfeiçoamento de Pessoal de Nível Superior (CAPES), under project 1655506, and the Fundação de Apoio ao Instituto de Pesquisas Tecnológicas (FIPT).

6. REFERENCES

Abbott, I.H. and Von Doenhoff, A.E., 1959. *Theory of wing sections, including a summary of airfoil data*. Courier Corporation.

Anderson, J.D. and Corda, S., 1980. "Numerical lifting line theory applied to drooped leading-edge wings below and above stall". *Journal of Aircraft*, Vol. 17, No. 12, pp. 898–904.

Anderson Jr, J.D., 2010. *Fundamentals of aerodynamics*. Tata McGraw-Hill Education.

Applin, Z.T., 1995. *Pressure distributions from subsonic tests of a NACA 0012 semispan wing model*, Vol. 110148. National Aeronautics and Space Administration, Langley Research Center.

Barnes, J.P., 1997. "Semi-empirical vortex step method for the lift and induced drag loading of 2d or 3d wings". *SAE transactions*, Vol. 106, pp. 1600–1617.

Chreim, J.R., 2016. "Extended lifting-line theory for viscous effects". `https://caaeroufabc.wixsite.com/home/copia-estagios`.

Committee, V.. *et al.*, 2009. "Standard for verification and validation in computational fluid dynamics and heat transfer". *American Society of Mechanical Engineers, New York*.

Eça, L. and Hoekstra, M., 2006. "Discretization uncertainty estimation based on a least squares version of the grid convergence index". In *Proceedings of the Second Workshop on CFD Uncertainty Analysis, Instituto Superior Tecnico, Lisbon, Oct*.

Hunsaker, D. and Phillips, W.F., 2011. "A numerical lifting-line method using horseshoe vortex sheets".

Katz, J. and Plotkin, A., 2001. *Low-speed aerodynamics*, Vol. 13. Cambridge university press.

Owens, D.B., 1998. "Weissinger's model of the nonlinear lifting-line method for aircraft design". *AIAA paper*, pp. 98–0597.

Phillips, W. and Snyder, D., 2000. "Modern adaptation of prandltls lifting-line theory". *Journal of Aircraft*, Vol. 37, No. 4.

Prössdorf, S. and Tordella, D., 1991. "On an extension of prandti's lifting line theory to curved wings". *IMPACT of Computing in Science and Engineering*, Vol. 3, No. 3, pp. 192–212.

Rumsey, C., Smith, B. and Huang, G., 2012. "Langley research center turbulence modeling resource - 2dn00: 2d naca 0012 airfoil validation case". `http://turbmodels.larc.nasa.gov/naca0012\_val.html`. Accessed: 2017-09-13.

Van Dam, C., Vijgen, P. and Holmes, B., 1991. "Experimental investigation on the effect of crescent planform on lift and drag". *Journal of aircraft*, Vol. 28, No. 11, pp. 713–720.

Weissinger, J., 1947. "The lift distribution of swept-back wings".

Wickenheiser, A.M. and Garcia, E., 2007. "Aerodynamic modeling of morphing wings using an extended lifting-line analysis". *Journal of Aircraft*, Vol. 44, No. 1, pp. 10–16.

Wickenheiser, A.M. and Garcia, E., 2011. "Extended nonlinear lifting-line method for aerodynamic modeling of reconfigurable aircraft". *Journal of Aircraft*, Vol. 48, No. 5, pp. 1812–1817.

7. RESPONSIBILITY NOTICE

The authors are the only responsible for the printed material included in this paper.